BUI

NO.65
(1987)

BUILDING RESEARCH ASSOCIATION OF NEW ZEALAND

REPRINT

Cl/SfB

h : i (L44)

UDC 691.7:691.11:674.04:620.193

Electrochemical study of the corrosion of metals in contact with preservative-treated wood

E.J. Jack and S.I. Smedley

(This report was commissioned by BRANZ as part of its ongoing research into corrosion problems. The views represented are not necessarily those of the Association.)

BUILDING RESEARCH ASSN. OF N.Z.
- 4 NOV 1987
LIBRARY
PRIVATE BAG PORIRUA
N.Z.

Reprinted from ***Corrosion***,
Vol.43, No.5 (1987)

BUILDING RESEARCH ASSOCIATION OF NEW ZEALAND

Am 23525
B 14832

Electrochemical Study of the Corrosion of Metals in Contact with Preservative-Treated Wood*

*E. J. JACK and S. I. SMEDLEY**

Abstract

An electrochemical study has been made of the corrosion of iron, zinc, and copper in contact with copper-chromium-arsenic (CCA) preservative-treated pinus radiata as a function of treatment level and moisture content. The techniques used were AC impedance, linear polarization, and weight loss measurements. They reveal that the corrosion rate is probably diffusion controlled and below 22 wt% of water, dependent on the moisture content. The results also indicate that there is probably a relationship between the corrosion rate and degree of preservative loading.

Introduction

Because of the predominance of exotic softwoods in New Zealand, preservative-treated pinus radiata has become a commonly used building material. One of the most frequently used preservatives is copper-chromium-arsenic (CCA), which is highly effective in resisting fungal attack and insect pests. However, it is known that the salt formation treatment enhances the corrosion rate of metal fasteners in contact with the timber and that this is further exacerbated as the moisture content of the wood is increased. These findings are based on weight loss, resistivity, and quantitative visual observation techniques and are well surveyed in a recent publication by Bailey and Schofield.[1] The corrosion mechanisms are generally assumed to be:

1. In untreated timber by differential aeration that, because of increased wood resistance, becomes effective below ~20% moisture content, and by acetic acid in the wood; and

2. In treated timber by differential aeration, although to a lower moisture content because of the enhanced conductivity, and by pitting corrosion as a result of the reduction of Cu onto the metal surface and hence the establishment of galvanic corrosion cells. This process may also be limited to a certain minimum moisture level for a significant amount of corrosion to occur.

Metal-Wood Electrochemical System

Most electrochemical investigations are concerned with the reactions that occur upon the contact of a metal and a homogeneous isotropic electrolytic medium, either solid or liquid. Wood is neither homogeneous nor isotropic; its structure is complex and will therefore be expected to have some effect on the rate of reactions occurring in the interfacial region upon the contact of metal and wood.

In the axial direction, pinus radiata is comprised almost entirely of tracheids, or long, open cells that fulfill the functions of providing mechanical support and mass transfer of fluids up and down the tree.[2] Thus, the transverse section (a plane at right angles to the axial direction of the tree) appears to be constructed of a bundle of pipes. Both longitudinal sections, radial and tangential, illustrate the longitudinal character of these pipes and appear similar, but very distinct. from the transverse section.

Water is absorbed into dry wood by incorporation into the cell walls until the fiber saturation point is reached at ~30 wt%. Beyond this level, the water enters the tracheids. It is reasonable to expect that beyond 30% water content, ionic transport will be easier in the axial direction (along the tracheids) than the radial direction, but below this level, their electrical conductivities will be similar. The presence of water will enhance the hydrolysis of acetylated polysaccharides to produce acetic acid. Preservation of timber using a salt formation CCA mixture introduces soluble species such as Cu^{2+}, Na^{+}, and $SO_4^{=}$ ions, which can also be carried by this solution.

It is probable that when in contact with a metal, wood promotes corrosion by (1) providing an electrolyte medium that can transport reactants to and products from the metal surface and (2) providing a source of H^{+} ions from the products of the hydrolysis of acetylated polysaccharides and other reducible species such as Cu^{2+}. Clearly, the presence of water will enhance corrosion by (1) and (2), and grain direction will have a significant effect on (1), at least at high moisture levels.

Thus, with the above discussion in mind, a thorough study of the corrosion of metals by wood should at least include experiments to determine the effect of (1) grain orientation, (2) water content, (3) atmospheric composition, (4) supporting electrolyte, (5) the passage of time, and (6) additional electrochemically reducible ions on the corrosion rate of a metal. It is clearly impractical to cover all of these variables over the whole range of conditions, but it is important to obtain an idea of the significance of (1), (3), and (4) before commencing a more thorough study of the effects of (2), (5), and (6).

* Submitted for publication August 1985; revised July 1986.

* Chemistry Dept., Victoria University of Wellington, Private Bag, Wellington, New Zealand.

Reprinted from CORROSION, Vol. 43, No. 5, pp. 266-275 (1987) May

Copyright 1987 by the National Association of Corrosion Engineers, P.O. Box 218340, Houston, Texas 77218

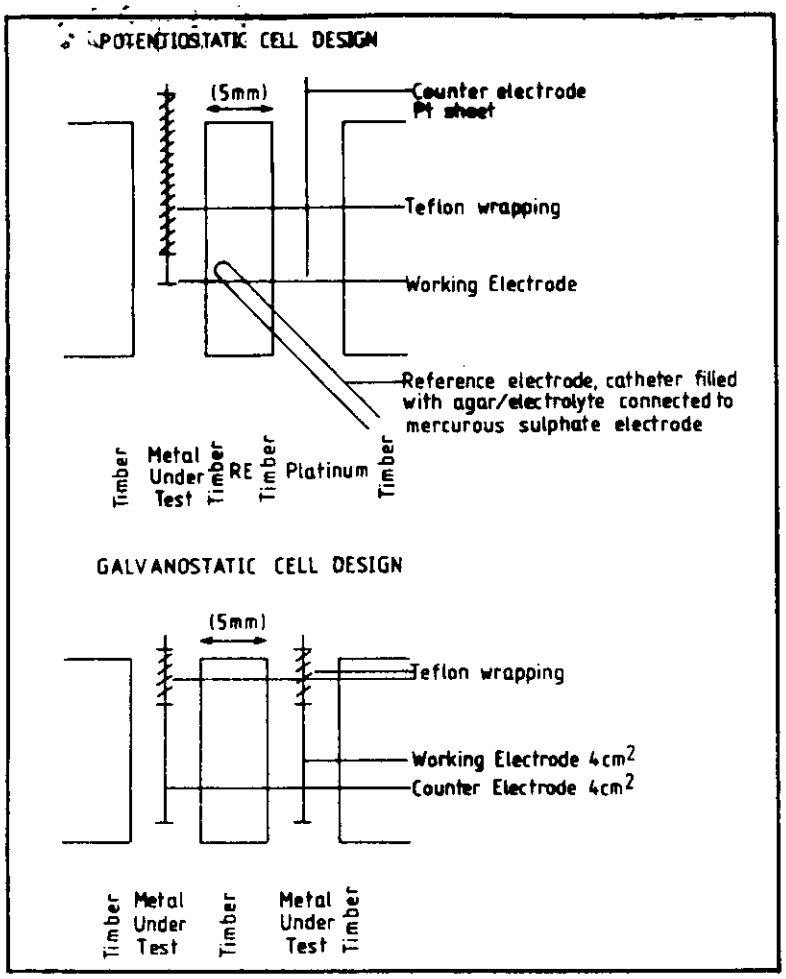

FIGURE 1 — Diagram of the potentiostatic and galvanostatic cells.

The objective of this work was to use the AC impedance measuring technique to study the corrosion of metals in contact with wood as a function of the metal, degree of preservative loading, and moisture content of the wood. It was envisaged that the impedance of the corroding system would be a complex function of frequency, but that it would be possible to extract information from the impedance spectrum, which would enable identification of a parameter that was proportional to the corrosion rate.

Experimental Method

In this study, AC impedance, DC steady-state, weight loss, and potential measurements were performed on the corrosion cell. The corrosion cells were of a sandwich construction with slices of wood clamped between metal electrodes. Both galvanostatic and potentiostatic cells were developed.

Cell Construction

Potentiostatic cells. Figure 1 shows a diagram of a potentiostatic cell. The working electrode was constructed from the metal under testing and was wrapped in Teflon[1] tape to expose a predetermined area to the wood. The reference electrode was $Hg\text{-}Hg_2SO_4\text{-}H_2SO_4$ (0.5 M) prepared in the manner of Beck, et al.,[3] and the counter electrode was made from sheet platinum. Contact between the reference electrode and wood was made via a catheter filled with Na_2SO_4 and agar, which was inserted into a small hole drilled into the wood ~0.15 cm from the working electrode. This procedure provided good electrical contact, especially if the wood had a high moisture content. The present authors experimented with working electrodes of increasing size to establish the maximum area that would produce an impedance response that was inversely proportional to the area. The area was 0.5 × 0.5 cm for most cells. Electrodes larger than this produced an impedance response, as measured by the distance between the low- and high-frequency intercepts on the real axis, that was not proportional to the electrode area. The potentiostatic cell had disadvantages in that it would not operate successfully with wood samples below ~23% moisture content and that the small electrode area made the results very susceptible to discontinuities in the wood.

Galvanostatic cells. Galvanostatic cells consisted of a wood sample sandwiched between two identical 2- × 2-cm electrodes (see Figure 1). Preliminary experiments revealed that the ratio of the impedance response between the potentiostatic cells of electrode area 0.5 cm^2 and galvanostatic cells was approximately in proportion to the area of the electrodes.

The electrode materials used (iron, zinc, and copper) were Johnson and Matthey[2] Grade 1. The metals were abraded with sandpaper (800 to 1200 grade) and cleaned in acetone. Iron electrodes were then dipped in 0.5 M H_2SO_4 for 10 min, which resulted in a clean, smooth surface. Zinc electrodes were dipped in 2 M HCl for 1 min, and the copper was etched in 30% HNO_3 for 30 s. The metals were then thoroughly rinsed in distilled water.

Wood Preparation

Untreated and CCA-treated samples of pinus radiata at C2 and C7 loadings were supplied by the Forest Research Institute of New Zealand.[4] These were prepared in accordance with the specification in Reference 4, and analysis revealed the elemental loadings, expressed as a percentage of oven dry weight, to be as follows: for Sample 1, the copper, chromium, and arsenic levels for the C2- and C7-treated wood were 0.36, 0.36, 0.65, and 0.13, 0.14, 0.42, respectively; those for Sample 2 wood were 0.22, 0.19, 0.34, and 0.09, 0.08, and 0.14, respectively.

The wood was stored for 2 months after it was received to ensure copper fixation; it was then dried in an oven at 100 C. Dry wood was then cut into slices with a band saw, and the faces were turned on a lathe to produce smooth plane parallel sides. Wood slices were brought to a constant moisture level by equilibration with the vapor of a saturated salt solution for ~2 weeks before cell construction. The percentage of moisture content calculated as percentage moisture content

$$= \frac{100 \times (\text{weight at test} - \text{weight after drying})}{\text{weight after drying}}$$

were assumed to be those given from the calibration table in Reference 5.

Electrochemical Apparatus

Measurements of the impedance of the corroding system were made between 10 kHz and 0.1 mHz using a Solartron/Schlumberger 1174[3] frequency response analyzer (FRA) connected to a PAR Model 173[4] potentiostat and PAR Model 179[5] coulombmeter or a PAR Model 276[6] interface. A sine wave of 10 mV root mean square (rms) generated by the FRA was fed into the summing junction of the potentiostat control amplifier; the voltage and current response of the cell taken from the potentiostat were fed into the x and y inputs of the FRA. The transfer function at each frequency was transferred from the FRA to an HP 85A[7] microcomputer and the results displayed as impedance on a Nyquist or Bode diagram.

There was concern that the high electrolyte resistance that would be encountered in these experiments would produce extraneous high-frequency phase shifts. Accordingly, the measuring system was tested with a number of potentiostatic and galvanostatic dummy cells to correlate the cell resistance characteristic with these high-frequency phase shifts. In most cases, the extraneous phase shifts became negligible below 1 kHz, below the time constants of the interfacial impedances.

The corrosion cells constructed from wood of a low

[1]Registered trade name.

[2]Johnson and Matthey, Royston, Herts, England.

[3]-[7]Registered trade names.

moisture content had a high resistance ($\sim 10^7\ \Omega$) and, hence, a very long time constant. Thus, to obtain the low-frequency intercept of the impedance curve with the real axis, it was necessary to run an impedance sweep for ~24 h. However, experiments that were conducted over this length of time exhibited a substantial drift in the impedance. Therefore, steady-state polarization resistance measurements were conducted to obtain a low-frequency intercept value for the impedance. The HP 85A microcomputer, interfaced to the potentiostat via the interface, was used to step the current at predetermined intervals and, after a predetermined time interval, to sample the cell voltage. The time interval was determined by the time required for the voltage to increase to 99% of its steady-state value, which is 4.6 τ/s, where τ is the time constant of the circuit and is determined from the frequency at z'' max. The slopes of the steady-state current voltage curves were determined by linear regression and corrected for the cell resistance, which was determined from the impedance diagram.

Experimental Technique

Corrosion cells were assembled from wood and metal that had been prepared in the manner described above. During electrochemical measurements, the cells were contained under controlled humidity conditions within a closed, grounded copper box. The cells were stored in a closed container between measurements, again under controlled humidity conditions achieved by placing a beaker of the appropriate salt solution within the container.

At the completion of an experiment, the cell was dismantled, the surface of the wood and metal examined under a microscope, the metal cleaned of corrosion products using the ANSI/ASTM G1-72[6] procedure, and the weight loss determined. Some metal surfaces were also examined with an electron probe microanalyzer to determine the nature of the corrosion products that adhered to the metal surface.

Results and Discussion

AC impedance and steady-state current potential measurements were conducted on galvanic cells constructed from untreated, C2, and C7 wood samples for iron, zinc, and copper. For cells constructed with iron and zinc, as well as some that were saturated in water, the range of moisture contents was from 12 to 28%; for copper cells, the range was 14 to 18%. A similar series of measurements was conducted on potentiostatic cells, but only for wood that had been saturated or was at a 27% moisture level.

Preliminary Experiments

Potential measurements. Potential measurements were made for iron in contact with untreated and C7- and C2-treated wood of saturated 27 and 21% moisture contents and in oxygen free nitrogen (OFN) and oxygen. Unfortunately, the potential variation of ~100 mV from one cell to another was sufficient to mask any trend in the potential as a function of preservative treatment level, but it was clearly dependent on the O_2 concentration. For example, one cell containing C2-treated wood saturated with water yielded an initial OFN reading of −868 mV with respect to the sulfate electrode, rose to −744 mV in oxygen, and then dropped again to −904 mV in the presence of OFN. This trend is equivalent to what would be expected for iron immersed in an aqueous solution, yielding a potential of ~ −0.200 mV with respect to the standard hydrogen electrode (SHE). Similar results were observed for cells constructed from wood of 27% moisture content; however, as the moisture level was reduced, the potential became more positive, but the potential measurements became less reliable.

Potential measurements were also conducted for zinc in contact with wood. The general conclusions were identical to those made for iron, with typical potential values being ~ −1200 mV with respect to the sulfate electrode or ~300 to 400 mV negative of iron, as would be expected on the basis of their standard electrode potentials.

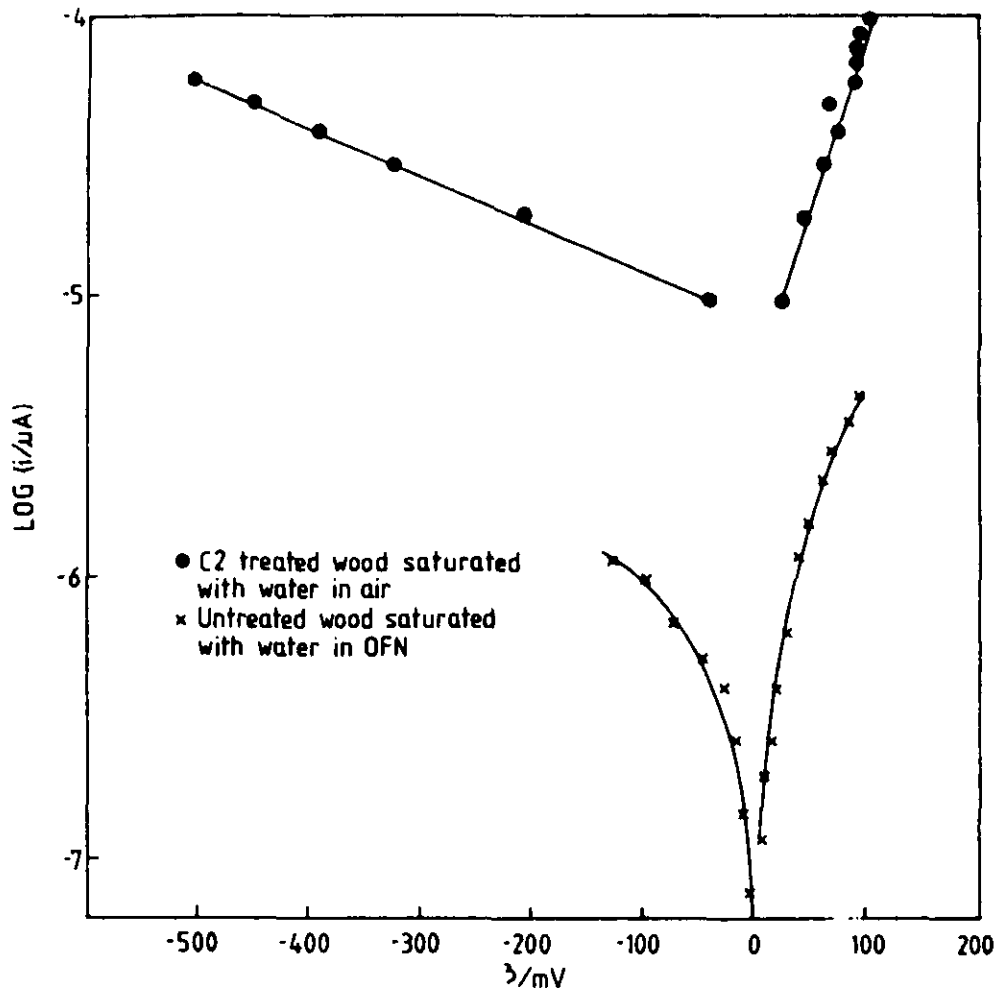

FIGURE 2 — log i vs overpotential for iron in contact with water-saturated wood.

Steady-state Tafel slope measurements. Steady-state current potential measurements were conducted on a number of cells. Figure 2 shows Tafel plots for two such cells. They indicate that the current is under cathodic control for these two cells. It is postulated that this probably results from the slow diffusion of reducible species such as O_2, H^+, or Cu^{2+}. Linear diffusion theory would predict that the cell current would approach a constant value in the presence of excess supporting electrolyte. However, the concentration of supporting electrolyte in the wood is low, ~0.2 mol dm^{-3} of Na_2SO_4 in C2-treated wood; hence, the measured total current will have a contribution from the migration current, which will always increase as the potential difference across the wood increases. Despite this complication, which is discussed in more detail below, the general conclusion of cathodic control for water-saturated cells seems reliable.

Impedance measurements. Figures 3 and 4 show impedance diagrams for iron in contact with treated and untreated wood in air and OFN. Some of these diagrams have the characteristic shape of impedance curves that arise from diffusion-controlled processes, and the data were successfully fitted to the circuit shown in Figure 3.

For the case in which there is an excess of supporting electrolyte, the Warburg impedance is given by

$$Z_W = \sigma_1 \omega^{-1/2} (1 - j) \tanh [\delta_1 \omega^{1/2} (\frac{j}{D_i})^{1/2}] \quad (1)$$

where the Warburg coefficient (σ_i) is given by

$$\sigma_i = \frac{RT}{\sqrt{2} n^2 F^2 C_i D_i^{1/2}} \text{ and } K = \delta_i (2/D_i)^{1/2} \quad (2)$$

where D_i is the diffusion coefficient of i, C_i is the concentration of i, and δ_i is the diffusion layer thickness. Estimates of σ_i and K were obtained from the impedance diagrams[7] and, along with values of C_1 and C_2, the double layer capacitances, and R_1 and R_2, the charge transfer resistances, were combined into an expression for the impedance of the equivalent circuit.

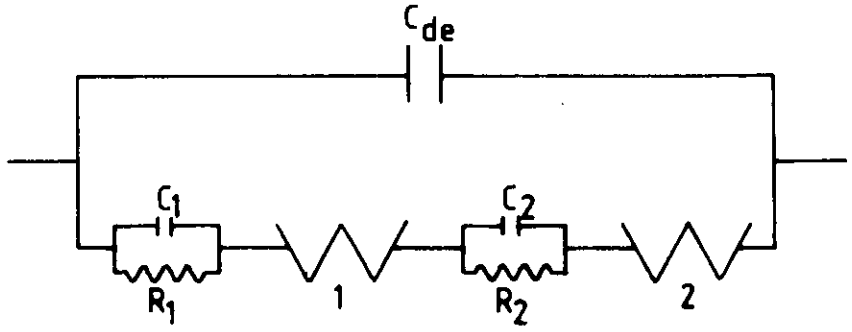

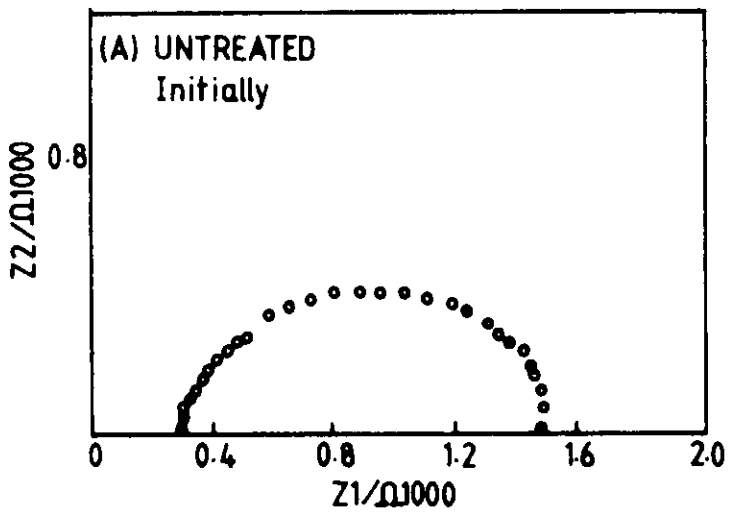

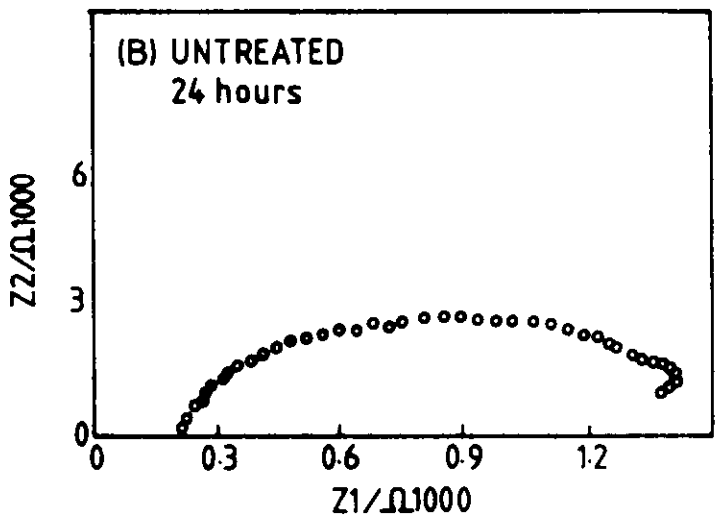

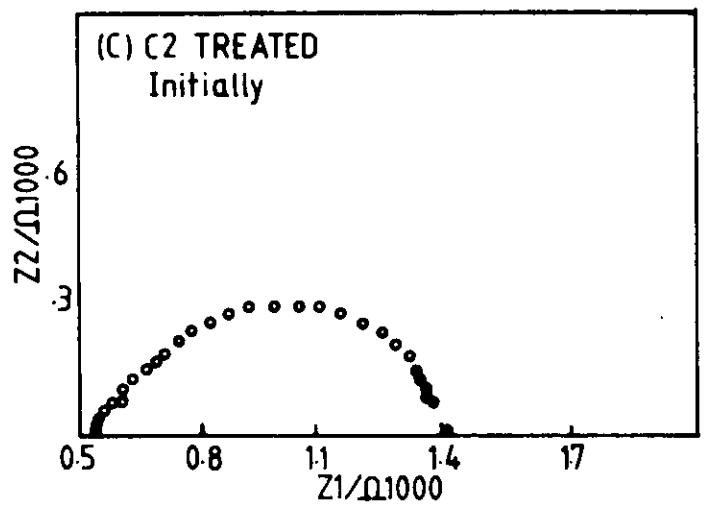

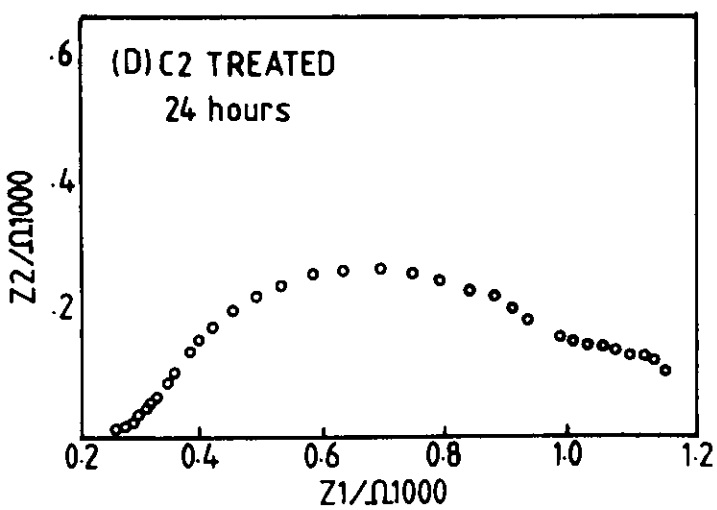

FIGURE 3 — Impedance diagrams for iron potentiostated at the corrosion potential and in contact with transverse section water-saturated wood in air. The equivalent circuit parameters are:

Cell	(a)	(b)	(c)	(d)
R_1/Ω	1	1	1	1
R_2/Ω	1	1	1	1
C1/μ F	5	5	5	5
C2/μ F	5	5	5	5
K1/$s^{1/2}$	0.1	0.69	0.6	0.64
K2/$s^{1/2}$	0.08	0.15	0.4	2.8
S1/Ω m^2 $s^{-1/2}$	6000	860	750	950
S2/Ω m^2 $s^{-1/2}$	6500	3733	1000	100
C	0	0	0	0

Note: electrode area = 0.25 cm^2.

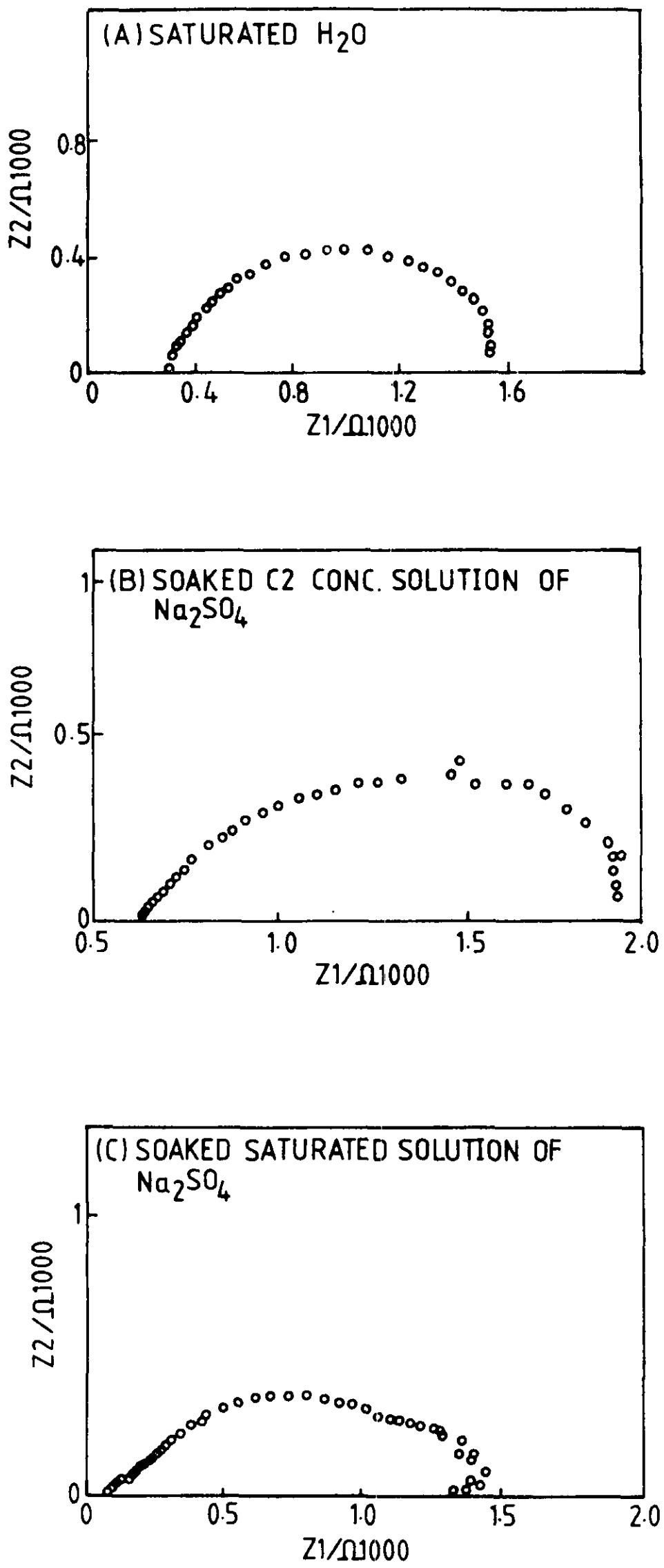

FIGURE 4 — Impedance diagrams for iron potentiostated at the corrosion potential in contact with transverse section water-saturated wood. The electrode area = 0.25 cm^2. The wood is untreated and, before cell assembly, was soaked in (a) H_2O, (b) Na_2SO_4 solution of the concentration expected to be found in C2-treated wood (i.e., ~0.1 mol dm^{-3}), and (c) in saturated Na_2SO_4 solution.

Bode plots were used to compare the fit of the simulated curves with that of the experimental ones. These plots were a more discriminating test than the impedance plane plots. A strong similarity of simulated and experimental curves was achieved, suggesting that the processes are diffusion controlled. It was not possible to simulate the impedance curves when the Warburg impedance was eliminated from the circuit diagram, although many different circuits were tried, thus indicating that the corrosion process is not kinetically controlled.

The best fit parameters are displayed with the circuit diagram and impedance plot in Figure 3. If, as assumed above, the process is under cathodic control, then the parameters presumably relate to the diffusion of O_2 and H^+ in untreated wood and to O_2, H^+, and Cu^{2+} in the treated wood. From these parameters and Equations (1) and (2), it is possible to obtain approximate δ_i and D_i values, given the O_2, H^+, and Cu^{2+} concentrations. However, the δ_i and D_i values obtained from these calculations do not vary with time or treatment level in a rational manner. The corrosion process is clearly more complicated than the simple analysis suggests; for example, it is likely that the three species H^+, Cu^{2+}, and O_2 are leading to the diffusional impedance, but it cannot be resolved into their separate contributions.

Apart from the general shape of the impedance diagrams, another parameter of interest is the distance (R_p) between the low- and high-frequency intercept of the impedance curve with the real axis. R_p is the interfacial impedance at zero frequency, i.e., the DC resistance of the interface at the applied potential. Therefore, at any potential, R_p should equal the resistance calculated from the gradient of the steady-state potential-current curve (corrected for cell resistance) at the same potential. From a different but identical cell used to collect the data shown in Figure 2 for the cell constructed from C2-treated wood, the following R_p values were obtained from the impedance diagrams. R_p = 1500 Ω at the rest potential, R_p = 800 Ω at 140 mV anodic overpotential, R_p = 9000 to 10,000 Ω at 100 mV cathodic overpotential, R_p = 900 Ω at 148 mV anodic overpotential, and R_p = 1800 Ω at the rest potential. These values compare well with the resistances (corrected for cell resistance) calculated from the data in Figure 2, i.e., R_p = 9500 Ω at 150 mV cathodic overpotential and 880 Ω at 100 mV anodic overpotential. The correspondence between the DC and AC results tends to confirm the conclusion that the corrosion process is controlled by the rate of the cathodic reaction, which is probably diffusion controlled.

Equation (1) for the Warburg impedance was initially derived for an electrode in the presence of an excess of an inert supporting electrolyte. In the absence of an excess of supporting electrolyte, a significant fraction of the current is carried by the migration of ions under the influence of the potential gradient. The migration current adds another term to the flux equation used to derive the Warburg impedance. A mathematical solution to this problem is being sought; however, in the mean time, several experiments were conducted to determine the significance of neglecting the migration term. Figure 5 shows the impedance diagrams for cells constructed from untreated timber that were saturated with water, Na_2SO_4 solution of the concentration that would be found in C2-treated timber, and saturated Na_2SO_4 solution. The impedance diagrams are shaped similarly to those referred to above, indicating that the reaction is diffusion controlled in all three cells. R_p, however, increases as the concentration of inert electrolyte increases. This could be explained by a diminution in the current (at constant potential) as the concentration of inert electrolyte increases. This would be expected since the migration current will diminish as more of the current is carried by the inert electrolyte. However, the effect of the excess of inert supporting electrolyte does not seem to be very significant, at least not sufficiently large to detract from the general conclusions made above.

In the presence of excess supporting electrolyte, the Stern-Geary[8] equation gives the relationship between the corrosion current (i), anodic and cathodic Tafel slopes (β_a and β_c), and polarization resistance (R_p):

$$i_{corr} = \frac{\beta_a \beta_c}{2.3\,(\beta_a + \beta_c)} \cdot \frac{1}{R_p} \qquad (3)$$

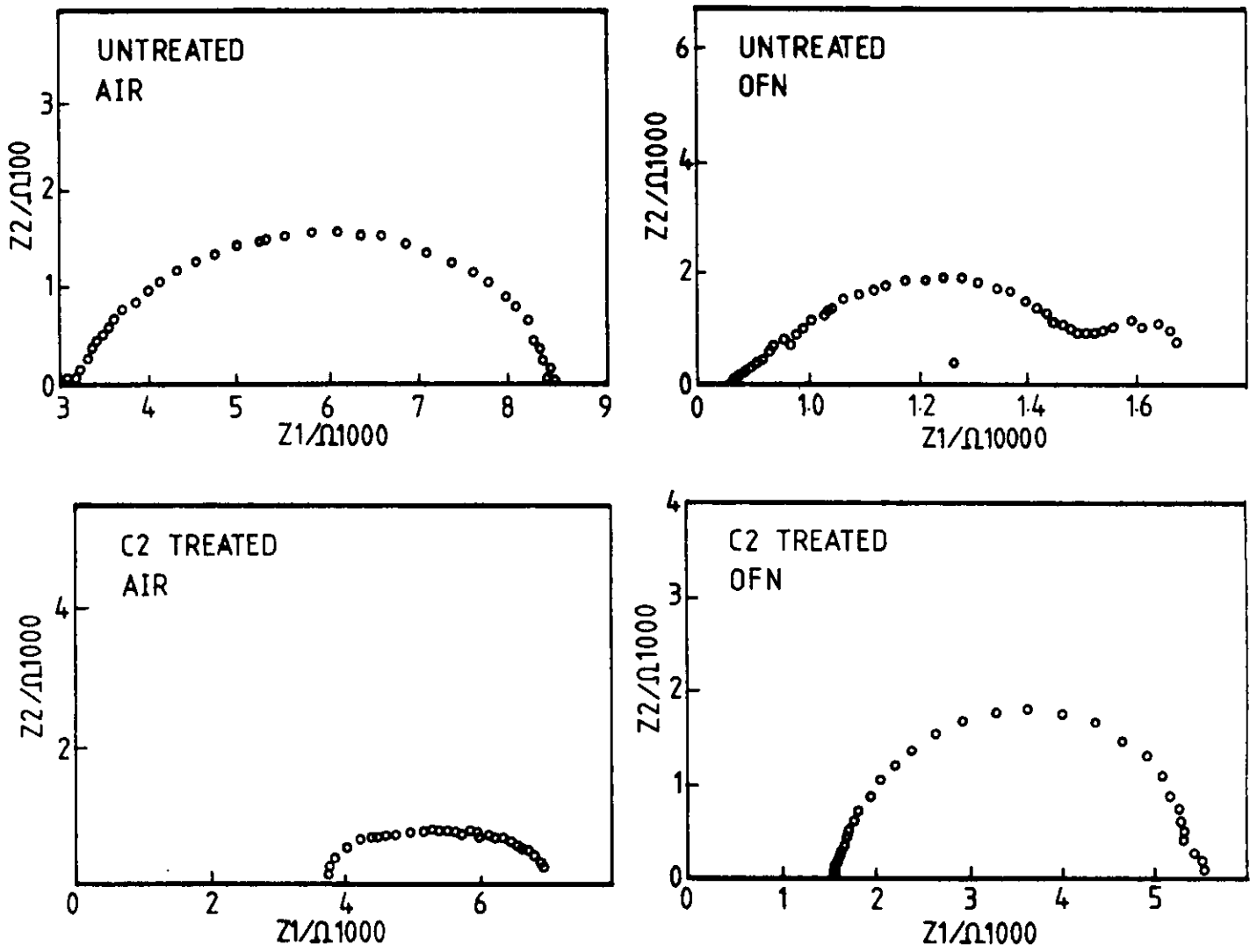

FIGURE 5 — Impedance diagrams for iron potentiostated at the corrosion potential in contact with water-saturated radial longitudinal wood in air and OFN. The electrode area = 0.25 cm².

For the case in which the process is diffusion controlled by the cathodic process, $\beta_c = \infty$,[9] and

$$i_{corr} = \frac{\beta_a}{2.3} \cdot \frac{1}{R_p} \tag{4}$$

R_p is the resistance to charge transfer at the electrode surface only, with the resistance resulting from the electrolyte having been specifically excluded. Therefore, the equation cannot predict the effect on the corrosion current that would arise from the resistance of the electrolytic current path between adjacent anodic and cathodic sites. In the case of pitting corrosion, this resistance is normally negligible because the path is so short, but it may become important in the case in which the electrolyte has a very high resistance, as in this work.

Considering a corrosion pit on the surface of a metal with adjacent anodic and cathodic sites, the potential difference (E) between these sites is given by

$$E = E' - \eta_a - |\eta_c| - i_{corr}R \tag{5}$$

where E′ is the open circuit potential; η_a and η_c are the anodic and cathodic overpotentials, respectively; and R is the electrolyte resistance. If the anodic and cathodic reactions are

$$M^{z+} + ze \rightleftharpoons M$$

and

$$X + ze \rightleftharpoons X^{z-}$$

then, at small overpotentials,

$$\eta_a = - \frac{RTi_{corr}}{nF} \left(\frac{1}{i_{o,a}} + \frac{1}{i_{\ell,M^{2+}}} \right) \tag{6}$$

and

$$\eta_c = - \frac{RTi_{corr}}{nF} \left(\frac{1}{i_{o,c}} + \frac{1}{i_{\ell,x}} - \frac{1}{i_{\ell,x^{z-}}} \right) \tag{7}$$

If the corrosion process is rate controlled, from Equations (5) through (7),

$$i_{corr} = E'/[\frac{RT}{nF} \left(\frac{1}{i_{o,c}} - \frac{1}{i_{o,a}} \right) + R] \tag{8}$$

If the cathodic reaction is diffusion controlled, then, in terms of charge (R_{ct}) and mass (R_{mt}) transfer pseudo-resistances,

$$i_{corr} = E'/[R_{ct} + R_{mt} + R_{mt} + R] = E'/[R_p + R] \tag{9}$$

$$= \frac{E'}{R_p} \times \frac{1}{(1 + R:R_p)} \tag{10}$$

For the experimental situations found in this work, in which the wood resistivity is large, R_p is also very large, so that the ratio of $R:R_p \cong$ constant; an approximate inverse linear relationship between i_{corr} and R_p is maintained under these circumstances. The constant relating i_{corr} to R_p may be calculated from mass loss data in the following manner.

The mass loss ($\triangle m$) of a corroding specimen can be related to the charge (Q_{corr}) passed during the exposure period by

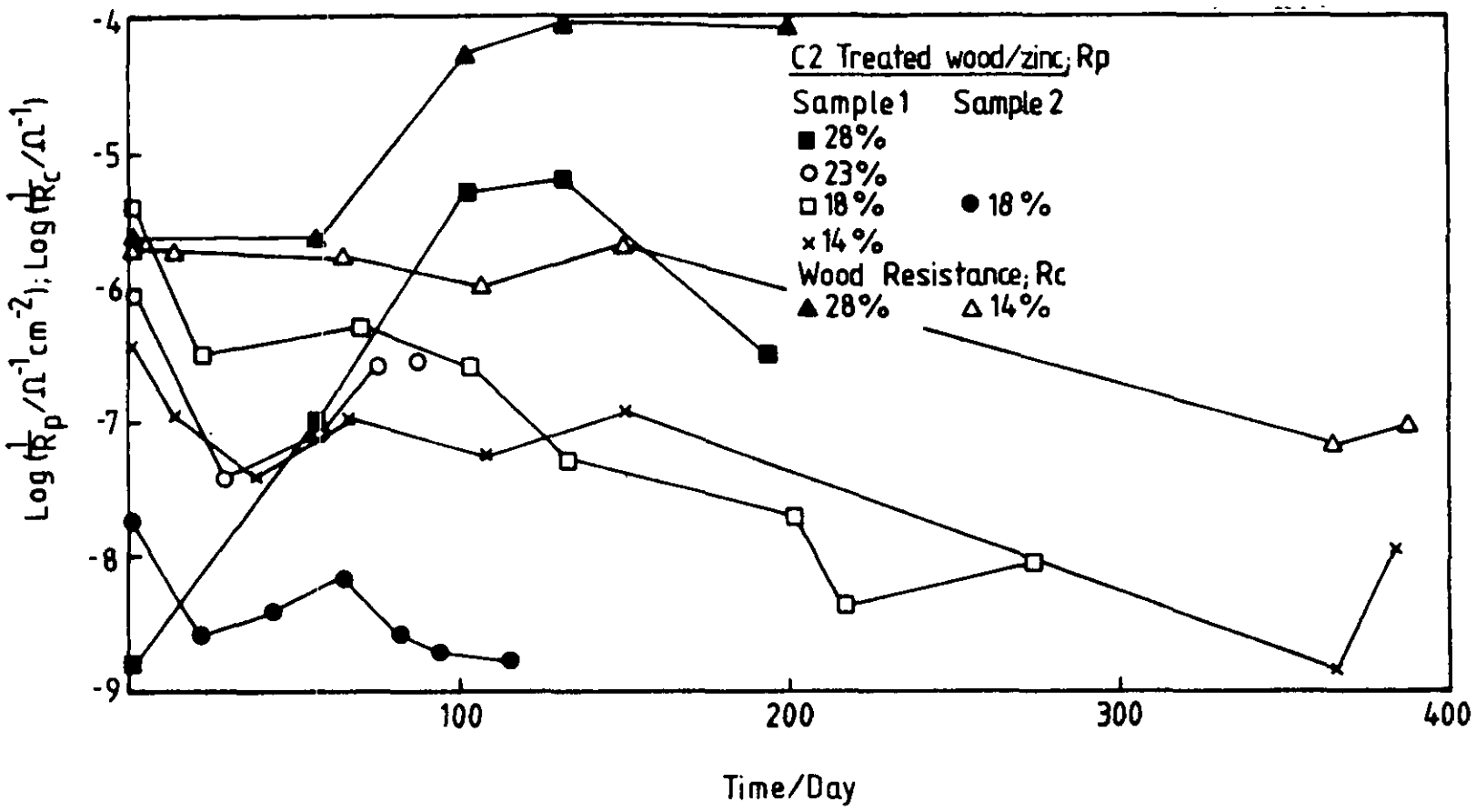

Time/Day

FIGURE 6 — Log R_p^{-1} (R_p = polarization resistance) and log R_c^{-1} (R_c = cell resistance) vs time for zinc in contact with C2-treated wood of different moisture levels.

$$\triangle m = \frac{Q_{corr} M}{nF} \qquad (11)$$

where M is the molecular mass. If i_{corr} is inversely proportional to R_p, $i = C{:}R_p$ where C is a constant. Since

$$Q_{corr} = \int_0^t i_{corr} dt = C \int_0^t \frac{1}{R_p} dt \qquad (12)$$

then C can be obtained by evaluating the integral. This can be conducted if R_p is known as a function of time.

Some further preliminary experiments can now be interpreted in light of the discussion above. They are:

1. *The effect of grain direction on the corrosion rate.* The present authors measured the impedance of cells constructed from iron on water-saturated untreated and C2-treated wood that had been cut so that the iron made contact with the transverse and radial and tangential longitudinal sections of the wood. R_p was significantly less for the transverse section (the grain direction at right angles to the face of the electrode) than for the other two directions, which is interpreted as meaning that the corrosion rate is therefore greater in this direction. This conclusion is reasonable for a diffusion-controlled reaction since O_2, Cu^{2+}, and H^+ diffusion is greater down the open tracheids than across them. All subsequent experiments were conducted with this grain orientation since it is the most corrosive and most technologically significant.

2. *Effect of O_2 on the corrosion rate.* For iron in contact with water-saturated, 28% moisture content-untreated, and C7- and C2-treated wood, R_p increases by a factor of ~ 2 when oxygen is removed from the system, indicating that the corrosion rate is halved (Figure 5). In the absence of oxygen, the cathodic current is presumably supplied by H^+ reduction and in treated timber, by Cu^{2+} reduction as well.

These experiments were conducted on iron in contact with saturated or 28% moisture content wood and illustrate that the wood behaves approximately as an anisotropic viscous electrolytic medium under these conditions. The corrosion reaction is controlled by the diffusion of cathodic reactants or products, and the corrosion current is inversely proportional to the polarization resistance, which is determined by the magnitude of the diffusion coefficients and the diffusion layer thicknesses.

For the above-mentioned reasons, a set of experiments similar to those described above could not be conducted on dry wood samples. However, the following evidence led to the belief that the above analysis for moist wood could be applied to dry wood. The faces of the drier wood samples (e.g., 14% that had been in contact with iron, zinc, and copper were impregnated with significant amounts of corrosion product sufficient to produce a barrier to diffusion. This conclusion was supported by the impedance diagrams for dry wood, many of which exhibited a straight line of approximately 45-degree slope. Further evidence is cited below in the discussion. Thus, it was assumed that for all of the corrosion cells studied in this work, the corrosion current is inversely proportional to the polarization resistance.

Long-Term Experiments

Impedance and polarization resistance measurements in the galvanostatic mode were conducted on Fe, Zn, and Cu in contact with untreated and C7- and C2-treated wood. The moisture levels ranged from 12 to 27%, and the experiments generally ran for a period of 100 to 200 days, with measurements being made at frequent intervals on each sample.

The polarization resistance was determined from the slope of the steady-state galvanostatic current-potential curve corrected for the cell resistance (R_c), which is given by the distance between the origin and high-frequency intercept of the impedance curve with the real axis. R_p values, so calculated, generally agreed with those obtained from the impedance diagram to within 20%, but some were as much as a factor of two different. However, in most cells in which the moisture level of the wood was below 20%, the low-frequency intercept could be obtained only by extrapolating the impedance curve. In these cases, the R_p value was taken to be that determined by the steady-state method. Figure 6 shows some representative plots of R_p against time. From this information and the mass loss experiments performed on each cell at the completion of a run, it was possible to evaluate the integrals in Equations (12) and (11) to obtain a value for the constant C and, hence, to calculate i_{corr}. Table 1 and Figures 7 through 10 give the data from these experiments and calculations.

Zinc

1. The mass loss data in Figure 10 illustrate two trends: increasing mass loss with increasing moisture level and, for

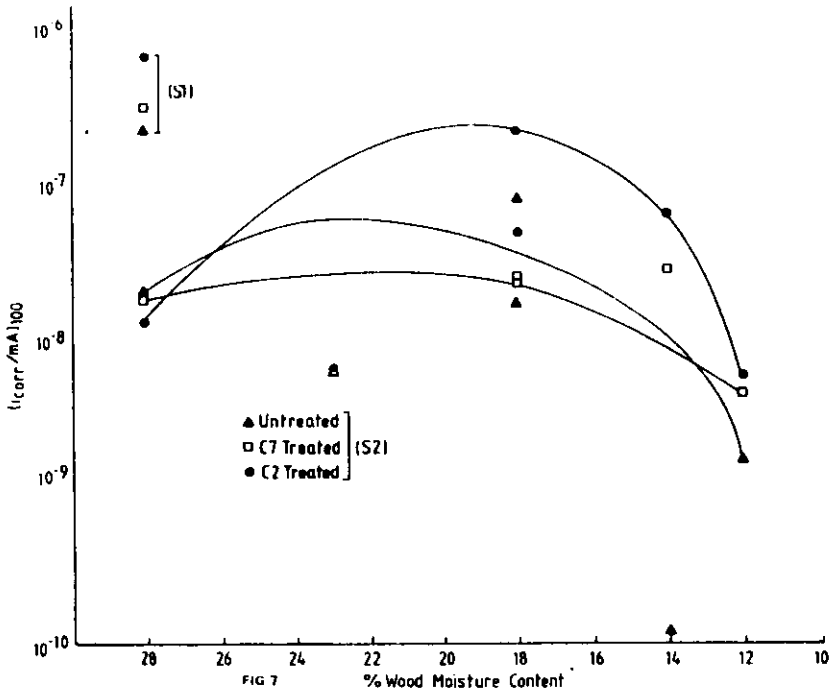

FIG 7

FIGURE 7 — Corrosion current vs wood moisture content for iron in contact with untreated and C2- and C7-treated wood after 100-day exposure. S1 and S2 refer to Samples 1 and 2 wood, respectively.

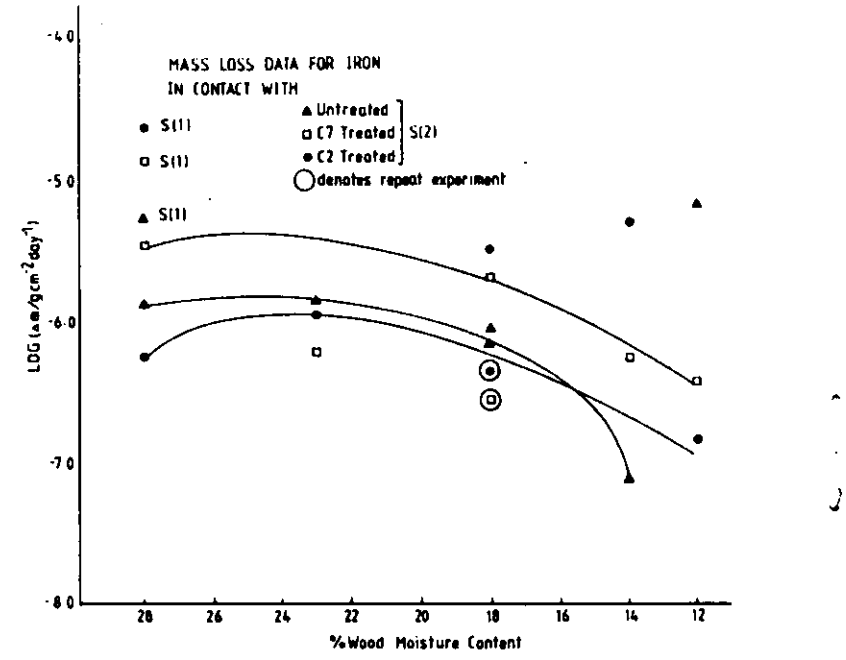

FIGURE 9 — Mass loss vs wood moisture content for iron in contact with untreated wood and C2- and C7-treated wood for Sample 2. S1 refers to Sample 1 wood.

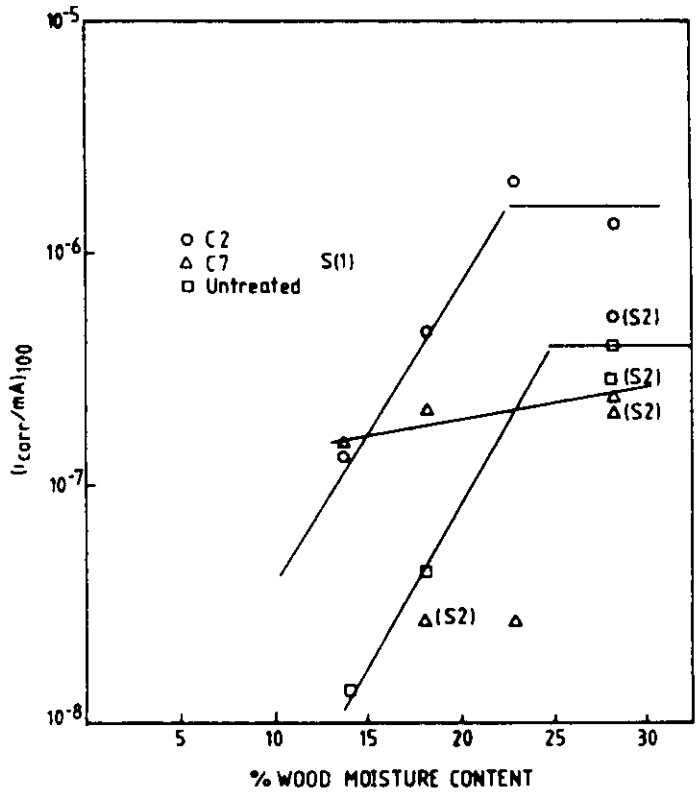

FIGURE 8 — Corrosion current vs wood moisture content for zinc in contact with untreated and C2- and C7-treated wood. S1 and S2 refer to Samples 1 and 2 wood, respectively.

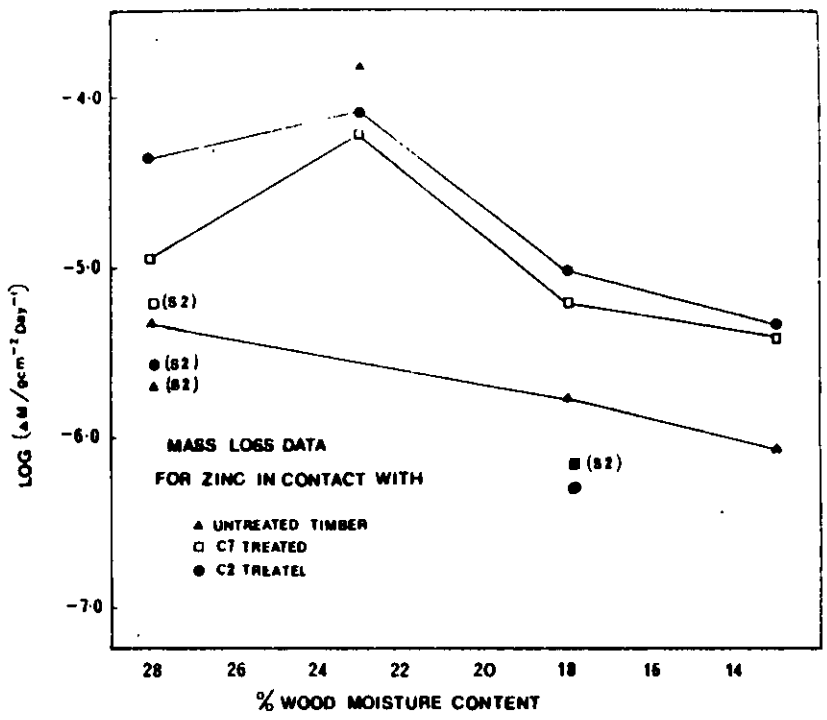

FIGURE 10 — Mass loss vs wood moisture content for zinc in contact with untreated wood and C2- and C7-treated wood from Sample 1. S2 refers to Sample 2 wood.

the Sample 1 cells, increasing mass loss with increasing treatment level.

2. The Constant C in Table 1 relating i_{corr} to R_p is much larger than would be expected if, as according to Equation (4), $C = \beta_a/2.3$. It exhibits a systematic variation with moisture content, being less dependent on the wood treatment level.

3. The corrosion currents at 100 days exhibit significant dependence on moisture content up to 23%; thereafter, they are approximately constant (Figure 8). The data for C7-treated timber are inconsistent with the pattern, which may result from the apparently random R_p fluctuations.

4. Samples 1 and 2 refer to cells constructed from different wood samples. R_c is consistently higher for Sample 2, indicating a lower conductivity, which presumably arises from the lower concentration of preservative salts in Sample 2 wood. The lower conductivity correlates with the higher R_p values and lower mass losses observed for cells constructed from this wood.

5. A common feature of all of the experiments (as shown in Figure 6) is that R_p fluctuates considerably; however, R_c values tend to follow these fluctuations. This indicates that a variable resistive component contributing to the cell resistance is also influencing the diffusion of reducible species to the metal surface. This could be caused by the growth of films on the electrode composed of corrosion products such as $Zn(OH)_2$ and $ZnSO_4$. The buildup of these would affect both R_p and R_c. R_p and R_c fluctuations will occur when these films periodically rupture and grow. R_p values for the C2-treated wood illustrate a definite trend toward higher values at long

TABLE 1 — Constant C in Equation (12) Obtained by Fitting to Experimental Data C/V

Metal	Zinc				
Moisture Content	28%	23%	18%	14%	12%
Wood treatment					
C2 (S1)	0.6	7.0	3.8	2.2	
C2 (S2)	1.3		3.7		
C7 (S1)	0.5	9.6	0.9	1.9	
C7 (S2)	2.9		13		
Un (S1)	1.2	4.0	1.0	1.0	
Un (S2)	2.2		11		
	Iron				
C2 (S1)	0.15			28	0.58
C2 (S2)	1.3	0.8	2.7, 28	28	0.58
C7 (S1)	0.2			9.6	1.9
C7 (S2)	1.6	1.2	11, 1.6	9.6	1.9
Un (S1)	0.5			0.06	9
Un (S2)	0.4	6.4	77, 9	0.06	9
	Copper				
C2 (S1)	3.3		0.05		
C7 (S1)	1.9		0.14		
Un (S1)	1.7				
	Mass loss/mg cm^{-2} day^{-1}				
C2 (S1)	4.1×10^{-7}		4.6×10^{-7}		
C7 (S1)	4.6×10^{-6}		3.1×10^{-7}		
Un (S1)	3.0×10^{-6}				
	i_{corr}/A at 100 days				
C2 (S1)	1.7×10^{-8}		1.2×10^{-8}		
C7 (S1)	1.1×10^{-7}		5.0×10^{-9}		
Un (S1)	1.3×10^{-7}				

times, suggesting that the electrode surfaces are becoming blocked with insoluble reaction products. This concurs with the observations of the metal and wood surfaces after the cells were dismantled where $ZnSO_4$ and $Zn(OH)_2$ deposits had formed; in some cases, these deposits cemented wood fibers firmly to the metal surface.

6. Table 2 gives surface analyses of zinc samples exposed to both untreated and C2-treated timber. They indicate that Cu was present on the surface of the zinc, in agreement with microscopic examination of the surface. It is significant that Cu was found, which must have resulted from the treated wood; the sulfur presumably results from $ZnSO_4$ deposits.

7. Visual examination of the zinc and wood surfaces on the disassembly of the cell revealed obvious signs of corrosion, except for those of the lowest moisture content. These signs were the formation of a white solid deposit on the wood and metal and the formation of pits. It was presumed that the deposit was $Zn(OH)_2/ZnSO_4$; the deposit had cemented wood fibers to the metal in some cases. Pits were formed on the metal in contact with the treated wood above 14% moisture content and in contact with saturated and 28% moisture content-untreated wood. Those surfaces that were not pitted exhibited a dull, gray surface. Some of the metal surfaces in contact with the saturated and 28% moisture content-treated wood had a black-brown color. This color surrounded the pits and was assumed to be copper deposits, as verified above.

Iron

1. The mass loss data in Figure 9 indicate a general trend of decreasing mass loss with decreasing moisture content. In common with the data for zinc, the mass loss appears to be approximately independent of moisture content above 23%. The data for Sample 1 cells at 28% moisture content indicate that the mass loss increases with increasing preservative loading, in common with the data for zinc, but this correlation is not apparent for Sample 2 cells. Furthermore, the results are not reproducible. The repeat measurements at 18, 15, and 12% moisture display large and anomalous variations from the other data. No explanation is given for these observations. The mass loss rates are lower for Sample 2 cells than for Sample 1 cells, again as observed for zinc electrodes.

2. The constant C in Table 1 does not vary significantly with treatment level, but tends to increase with decreasing moisture level. However, a systematic difference exists between the C values for Samples 1 and 2. The C value is much larger than would be expected on the basis of Equation (4).

3. Figure 7 shows the corrosion currents at 100 days; they reveal that the corrosion current is approximately constant from a 22% moisture level upward and decreases with decreasing water content below 22%. The data do not illustrate any clear dependence of the corrosion current on the preservative loading.

4. Table 2 gives surface analyses of iron samples exposed to both untreated and C2-treated timber. They indicate that copper was present on the surface of iron that had been in contact with treated timber. This concurs with some visual observations of the samples after dismantling the corrosion cells. The sulfur presumably comes from $ZnSO_4$.

5. Surface examination of the iron revealed that pitting and the formation of a brown corrosion product occurred on all samples. Furthermore, the iron samples in contact with saturated or 28% moisture content-treated wood had a coppery brown surface color that was assumed to be copper, as verified above.

TABLE 2 — Summary of Surface Analysis by Electron Probe Microanalyzer for Iron and Zinc

Iron		Zinc	
Treatment Level	Elements Present	Treatment Level	Elements Present
Untreated	Fe, S, Cl, As?,[1] Cu?	Untreated	Zn, S, Cl
C2	Fe, Cu, As?, S	C7	Zn, Cu, S
		C2	Zn, Cu, S, Cr, As?

[1]? signifies that levels were not conclusive.

Copper

1. The limited mass loss data indicate that the corrosion rate increases with increasing moisture content and, except for the C2-treated sample at an 18% moisture level, indicate that the mass loss rate is independent of the preservative loading. Similar conclusions can be drawn from the corrosion currents, which tend to be lower than those for corresponding zinc cells.

2. Both R_p and R_c tend to reflect the changes in the surface condition of the electrode with increasing time. They both increase with time, presumably as the electrode surface becomes blocked with corrosion products such as $CuSO_4$ and $Cu(OH)_2$. For the C2-treated sample at 18% moisture content, R_p is anomalously large—hence, the small mass loss for this cell. It is possible that the formation of corrosion products soon after assembly of the cell blocked further corrosion.

3. Examination of the copper surfaces revealed that all of the samples that had been in contact with treated wood had undergone pitting corrosion. All samples had formed a corrosion product that varied from green ($CuSO_4$) to bluish gray (CuO).

Conclusions

1. The corrosion rates of zinc and iron in contact with water-saturated wood are controlled by the diffusion of reactants to, or products from, the metal. It is likely that this conclusion extends to dry wood, in which the moisture content is 12% or more.

2. For saturated wood, the corrosion rate of the metal is approximately halved when oxygen is removed from the system, which implies that in the absence of oxygen, the cathodic current is carried by H^+ in untreated timber and H^+ and Cu^{2+} in treated timber.

3. The R_p values and hence corrosion currents vary significantly with increasing time. The corrosion rates of iron and zinc in contact with treated wood of 28% moisture content generally increase with time. The other samples exhibit the opposite behavior; the corrosion currents decrease with increasing time, which suggests that the processes are self-limiting. Since R_c follows the same trends, it is likely that the cause of these trends is buildup of corrosion products at the electrode surface. The copper electrodes seem particularly noticeable in this respect.

4. Figures 8 and 9 show that for all metals and for wood Samples 1 and 2, corrosion is distinctly dependent on moisture content below ~22% moisture content. The corrosion of iron and zinc in contact with wood of a 14% moisture level is ~8 to 10 times less than for iron or zinc in contact with wood of a 22% moisture level. The data for copper do not allow a firm conclusion to be drawn, but indicate that copper corrosion will follow a similar dependence on moisture level.

5. For zinc in contact with Sample 1 wood, the corrosion rate is dependent on the degree of preservative loading, with untreated wood being the least corrosive and C2-treated wood the most. The scant results for copper do not allow any reliable observations regarding the effect of preservative loading. The corrosion rates of zinc and iron in contact with Sample 2 wood do not exhibit an obvious trend as a function of preservative loading. Furthermore, the corrosion rates of iron and zinc in contact with Sample 2 wood are significantly lower than those for Sample 1 wood, with the difference being less for the untreated wood and greatest for C2-treated wood. The R_c values behave in a similar manner, with those for Sample 2 wood being up to 10 times greater. This difference presumably arises from the different preservative levels in the two wood samples, as discussed in the experimental section.

6. The corrosion rates of zinc, iron, and copper are similar, although the corrosion rates for copper are lower than those of zinc, which is to be expected if the enhanced corrosion of zinc when it is in contact with C2- and C7-treated wood results from the presence of free Cu^{2+} in the wood.

Acknowledgments

This research was conducted under the terms of a contract between Victoria University of Wellington and the Building Research Association of New Zealand. The authors thank J. Duncan of BRANZ for help and guidance during this project and J. W. Tomlinson of Victoria University for valuable assistance with certain aspects of developing the experimental technique and for helpful discussions of the ensuring results.

References

1. G. Bailey, M. J. Schofield, J. Inst. Wood Sci., Vol. 10, p. 14, 1984.
2. B. A. Meylan, B. G. Butterfield, Three-Dimensional Structure of Wood, Reed Education, Wellington, New Zealand, p. 80, 1972.
3. W. H. Beck, J. V. Dobson, W. F. K. Wynne Jones, Trans. Faraday Soc., Vol. 56, p. 1172, 1960.
4. Timber Preservation in New Zealand: Specifications, Revised ed., Timber Preservation Authority, Rotorua, New Zealand, 1969.
5. M. J. Cunningham, T. J. Sprott, Research Project R43, Building Research Association of New Zealand, 1984.
6. ANSI/ASTM G1-72, Part 10, ASTM, Philadelphia, Pennsylvania, p. 681, 1974.
7. J. L. Dawson, D. G. John, J. Electroanal. Chem., Vol. 110, p. 37, 1980.
8. M. Stern, A. L. Geary, J. Electrochem. Soc., Vol. 104, p. 56, 1957.
9. M. Stern, Corrosion, Vol. 14, No. 9, p. 60, 1958.

Printed in U.S.A.

Copy 2

B14832
0023525
1987
Electrochemical study of
the corrosion of metals i

BUILDING RESEARCH ASSOCIATION OF NEW ZEALAND INC.
HEAD OFFICE AND LIBRARY, MOONSHINE ROAD, JUDGEFORD.

The Building Research Association of New Zealand is an industry-backed, independent research and testing organisation set up to acquire, apply and distribute knowledge about building which will benefit the industry and through it the community at large.

Postal Address: BRANZ, Private Bag, Porirua

ISSN 0111–7459